Specie Concentration Measurements Utilizing Raman Scattering of a Laser Beam

GEORGE F. WIDHOPF* AND SAMUEL LEDERMAN†
Polytechnic Institute of Brooklyn Graduate Center, Farmingdale, N. Y.

The feasibility of utilizing Raman scattering as a diagnostic technique to measure individual specie concentrations in typical gas mixtures found in gas-dynamic applications has been investigated and demonstrated. Utilizing this technique, either the local density of a pure gas or the concentration of individual diatomic (or polyatomic) species in a gas mixture can be uniquely determined. The range and limitations of this technique were investigated and evaluated under controlled static conditions. A Q-switched ruby laser, which has a pulse duration of approximately 10 nsec, was used as a radiation source. Quantitative experimental results are given for some typical gases in their pure state, as well as in various mixture proportions.

I. Introduction

THE development of techniques capable of directly measuring local values of gas density has received much attention in recent years. This capability greatly enhances the information which can be experimentally obtained about gasdynamic flowfields, and could be of particular importance in situations where the determination of specie concentration or local density distributions are important. This is especially true when standard probe techniques interfere with the flowfield, or where the relative concentrations of the species being measured are altered by the sampling technique utilized.

Some techniques recently investigated included, electron beam fluorescence,[1,2] Rayleigh scattering,[3] and Thompson scattering.[4] Each has its own particular use and limitations.[5] There exists a need for a diagnostic technique which can complement the aforementioned techniques and possibly eliminate some of their inherent limitations. The investigation of such a technique is the subject of this paper.

When a beam of monochromatic light traverses a gas mixture, the resultant scattering phenomenon involves both the elastic and inelastic interactions of the photons with the gas molecules. The elastic interaction results in Rayleigh scattering, whereas that caused by the inelastic interaction results in Raman scattering. The Raman scattered radiation consists of radiation whose energy, and therefore, frequency has been changed by an amount characteristic of the energy differences between the stationary energy states of molecules it encounters. The shift can result in an increase in energy, and subsequent increase in frequency (Anti-Stokes Line), or a decrease in energy and subsequent decrease in frequency (Stokes Line), of the scattered radiation. This frequency shift is a unique characteristic of the scattering molecules and is independent of the frequency of the incident radiation. Therefore, the individual species present in the gas mixture can be uniquely distinguished by monitoring the frequencies of the scattered radiation. Not only can one distinguish between the different species comprising a gas mixture, but, by measuring the intensity of each component of the scattered light one can determine, in theory, the individual rotational and vibrational temperature and concentration of each diatomic or polyatomic species in the mixture.

Since the Raman effect is a scattering phenomenon, the only effect of the other species present in the mixture should be the attenuation (due to absorption or rescattering) of the resulting scattered radiation. Thus, the ability to detect and measure the concentration of a particular species in a mixture, should not be affected by the type or amount of other species present, provided proper precautions are taken in order to attenuate all other wavelengths present. This, of course, assumes that the subsequent attenuation due to the presence of other molecules is negligible (see Sec. IV). In the same manner, the presence of any dust particles will not affect these results, since the scattering from any dust particles is of the Rayleigh type or has its own characteristic frequency shift.

It is the intent of this investigation to use the Raman scattered radiation as a diagnostic tool in order to identify unknown species in a gas mixture, as well as to measure their concentration and vibrational temperature. This type of application has been previously proposed and described in the combined effort included in Refs. 6–8, wherein some exploratory experimental measurements were initiated. Raman scattering has also been proposed and used for probing the upper atmosphere.[9]

In this paper, the feasibility of utilizing Raman scattering as a diagnostic technique in the realm of gasdynamic measurements is to be experimentally determined. To achieve this end, a static calibration under controlled conditions was initiated. A review of the pertinent concepts describing the Raman effect is presented, together with quantitative experimental results. Specifically, its applicability and use under varying conditions, as far as gas density, discrimination ability in various gas mixtures, and loss factors are discussed and experimentally determined.

II. Theory

Consider a photon of arbitrary energy $h\nu_0$, which interacts with a molecule in one of its various stationary states characterized by a discrete energy level E. During the interaction between the molecule and the photon, the molecule undergoes a double transition, by first absorbing and then emitting a photon. During the absorption, the energy of the molecule is raised to $E + h\nu_0$, which may or may not be one of

---

Presented as Paper 70-224 at the AIAA 8th Aerospace Sciences Meeting, New York, January 19–21, 1970; submitted February 3, 1970; revision received August 10, 1970. Research conducted under Contract Nonr 839(38) for Project Strategic Technology, supported by the Advanced Research Project Agency through the Office of Naval Research. Taken from the dissertation submitted by G. F. Widhopf to the faculty of the Polytechnic Institute of Brooklyn in partial fulfillment of the requirements for a PhD in Astronautics, June 1970.

* Formerly Research Associate; presently, Member of Technical Staff, Fluid Mechanics Dept., The Aerospace Corporation, San Bernardino, Calif. Associate Member AIAA.

† Associate Professor of Aerospace Engineering. Member AIAA.

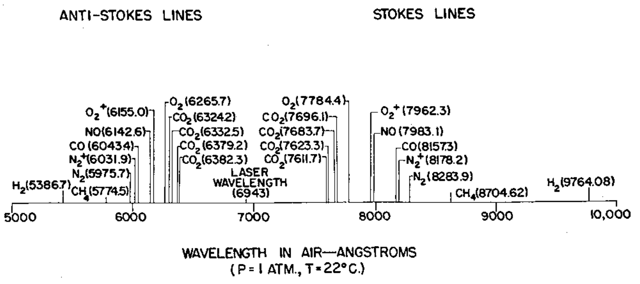

Fig. 1 Wavelengths of Raman scattered radiation for various molecules excited by a ruby laser (6943Å) as measured in air.

its stationary energy states. If this state does not correspond to a stationary state, the photon is scattered in some direction and the molecule falls to a lower energy level. If the molecule returns to its original state E, the energy and frequency of the scattered photon remains unchanged although its direction may be changed. This type of scattering corresponds to the aforementioned Rayleigh scattering. It is possible that the molecule does not return to its original unperturbed energy state E, but changes to a different energy level E_1. This will result in a corresponding change in the scattered photon energy. If $E_1 > E$, the energy of the photon is decreased to $h\nu_0 - (E_1 - E)$, while the internal energy of the molecule has been increased by $(E_1 - E)$. If $E_1 < E$, the energy of the photon is increased to $h\nu_0 - (E_1 - E)$ and the molecule's internal energy is decreased by $(E_1 - E)$. This latter process can only occur if E is not the ground state energy. Some of the scattered radiation is, therefore, of a different frequency than the incident radiation and is known as Raman scattering. The former process gives rise to what is usually termed the Stokes component, while the latter is termed the Anti-Stokes component of the Raman scattering. The time scale for Raman scattering to occur is approximately 10^{-14} sec.[10]

At any given temperature, the molecules in a small volume are distributed over their possible energy states. In thermal equilibrium they are distributed according to the familiar Boltzmann distribution. Therefore, there will always be some molecules in an energy state above the ground state. With this in mind, and remembering that each of the transitions previously described have a finite probability of occurring, it is evident that during any scattering process, Raman Stokes and Anti-Stokes as well as Rayleigh components should be expected to occur simultaneously. The intensity of each of these components will, of course, be different.

The intensity of these scattered radiation components can be determined utilizing the perturbation theory of wave mechanics.[11–13] Placzek[12] introduced the concept of a polarizability tensor ($\hat{\alpha}$) which, under certain conditions, simplifies the evaluation of the transition probability. This concept is useful, since the components of $\hat{\alpha}$ can be determined experimentally (see Ref. 5 for more details).

The transition probability amplitude is, in general, a function of the observation angle, the mode of polarization of the incident radiation as well as the specific type of transition under consideration. The vibrational and/or rotational transitions will be considered herein, since in practice almost all Raman spectra recorded results from these types of molecular transitions. The transition probability amplitude for the vibrational-rotational transition as a function of the observation angle, for linearly polarized and unpolarized incident radiation is given in Ref. 5.

In the experiments described herein, the incident radiation was vertically polarized and the entire vibrational-rotational Raman band was observed. Under these conditions, the intensity of the scattered radiation for an individual specie can be written in the following form:

$$I_{S,A} = C_2(\nu_0 \mp \nu)^4 N \frac{h}{8\pi^2 c\mu\omega_e} I_0 \left[\alpha'^2 + \frac{7}{45}\gamma'^2\right]\Omega \quad (1)$$

where $I_{S,A}$ are the Stokes and anti-Stokes intensities, respectively, watts; ν_0 is the wavenumber of the incident radiation, cm^{-1}; ν is the wavenumber of the vibrational Raman shift, cm^{-1}; N is the number of molecular scatterers; ω_e is the frequency of vibration in cm^{-1}; h is Planck's constant; μ is the reduced mass of the molecule; c is the velocity of light; I_0 is the intensity of incident radiation, watts/cm^2; Ω is the solid angle of the observation system; C_2 is a constant; α' is the isotropic part of the change of the polarizability; and γ' is the anisotropic part of the change of the polarizability. Both α' and γ' are molecular invariants.

It is seen from Eq. (1) that the intensity is dependent upon the number of scattering molecules, the frequency of the scattered radiation, the incident intensity and certain molecular constants.

The determination of the wavelengths of the various Raman components should be done with the greatest degree of accuracy (i.e., better than the resolution required in the investigation). This can be accomplished, for diatomic molecules, by utilizing the vibrating rotator molecular model as described in Ref. 14. The procedure, equations and molecular constants necessary for such a calculation are described and given in Refs. 5 and 14.

Utilizing these models the wavenumbers, in vacuo, of the Stokes and Anti-Stokes components can be computed for each species. Since the measurements are usually made in air, the index of refraction of air must be taken into account. The Raman wavelengths of some interesting species calculated utilizing this procedure are shown in Fig. 1. Included therein, are the wavelengths for the CO_2 and CH_4 Raman components as computed using the Raman shifts reported in Ref. 15.

The molecular invariants α' and γ', for a given species, should also be known. These invariants, as previously indicated, can be determined experimentally. Their exact measurement is a delicate and difficult task and many attempts have been made in the past to determine these constants.[15,16] Examining the available data for α' and γ', it was found that the work in Ref. 15 was very reliable. These results are expected to be accurate within the experimental error of this investigation and are listed in Table 1. The data from other investigations are given in Ref. 5, together with those used herein. Certain quantities needed for our calculations, which were derived from the data of Ref. 15, are included in Ref. 5.

Since the intensity of the scattered radiation depends upon the number of molecular scatterers present in the volume being investigated, a measurement of the intensity will give N or the concentration of the particular species under consideration. For any given situation both the Stokes and Anti-Stokes components should be present, therefore, theoretically, the intensity of either component could be used to determine the concentration of a particular specie. In practice, however, the Stokes line should be used, since it is usually more intense at the lower temperatures. Considering only the Stokes components of the Raman scattered radiation, Eq. (1) can be rewritten, including the attenuation factors introduced by the experimental apparatus, in the form,

$$\frac{I_{sp}}{I_0} = C_2 V N \varphi(T) \frac{(\nu_0 - \nu)^4}{\omega_e} \frac{h}{8\pi^2 c\mu} \left[\alpha'^2 + \frac{7}{45}\gamma'^2\right] \frac{A_1}{r^2} \frac{A_s}{A_i} L \ldots \quad (2)$$

Table 1 Molecular data and relative Stokes intensities

Specie	Raman shift	α'	$(\gamma'/\alpha')^2$	I_S/I_{SO_2}	I_S/I_{SO_2}	I_S/I_{SO_2}
	(cm^{-1})	(10^{16} cm^2)		(theory)	(spectro.)	(filters)
O_2	1556.2	1.46	4.02	1.0	1.0	1.0
N_2	2330.7	1.75	1.71	0.668	0.643	0.74
CO_2	1265 1285 1388 1409	4.20	1.26	1.97	2.32	1.87

where I_{sp} is the intensity of the scattered radiation from an individual specie as seen by the phototube; V is the scattering volume, cm^3; N is the specie molecular concentration, particles/cm^3; $\varphi\ (T)$ is the percentage of the molecules which are in the ground state at the temperature T; thus, $\varphi\ (T)\ NV$ is the number of molecular scatterers present in the sampling volume; A_l is the collecting lens area, cm^2; r is the distance between the scattering center and the collecting lens, cm; A_s is the illuminated area of the slit, cm^2; A_i is the area of the image of the scattering volume on the spectrograph slit, cm^2; L is the transmission factor of all the optics (lenses, filters, grating, etc.) in the system.

Equation (2) gives the functional dependence of the scattered intensity upon the various governing independent parameters. It is important to note the linear dependence with number density. Theoretically, a measurement of I_0 and I_{sp}, knowing all other quantities, will yield the number density of the species under consideration.

Taking the ratio of the intensities of the Stokes and Anti-Stokes components, and utilizing the Boltzmann distribution to determine the number of molecules in each vibrational state, results in

$$I_S/I_A = \frac{(\nu_0 - \nu)^4}{(\nu_0 + \nu)^4} \exp[ch\nu/kT] \tag{3}$$

where I_S and I_A are the intensities of the Q-branch.[5]

Since the frequency shifts have been determined previously, a measurement of I_A and I_S will determine the vibrational temperature when substituted in Eq. (3). It must be remembered that the utilization of the Boltzmann relation assumes thermal equilibrium, an assumption which may be violated in some applications.

As seen in Eq. (2) and Table 1, the Raman cross sections are very small, and therefore, in relatively short duration measurements, a high-intensity source is needed to produce scattered light of sufficient intensity which can be recorded above the local background and instrument "noise." The use of a Q-switched ruby laser (10 nsec pulse duration) satisfies this requirement and, in addition, permits the application of this technique in a dynamic situation.

III. Experimental Facility

The system characteristics given prime consideration in the design of the experimental facility were safety, elimination of unwanted reflections, and system versatility. The system (see Fig. 2) was therefore designed so that the laser radiation would be completely enclosed (where possible) in order to avoid any accidental observation of the laser radiation. These enclosures did not interfere with the experimental measurements and were designed for quick adjustment and removal.

Since the intensity of the Raman components of the scattered radiation is low, care must be taken in both its detection and measurement. Reflections of scattered and incident radiation into the viewing system must be avoided. This is particularly true if local measurements are to be made. The aforementioned statements are applicable for the Rayleigh components as well. Here, it is especially important, since the intensity of the Rayleigh component is normally at least three orders of magnitude larger than the Raman component and must be filtered out in order to avoid masking the Raman component.

To accomplish this, a radiation absorption chamber (see Fig. 2) was constructed and placed in line with the incident radiation direction. This provided a terminal for the incident radiation, wherein all radiation is internally reflected and absorbed within the chamber. A second chamber provided a good background for the viewing system.

The absorption chambers were designed similar to those utilized in Ref. 4, since they were easy to construct and proved very successful, in that investigation, in eliminating unwanted reflections. The chambers consisted of black anodized aluminum cylinders. The opening to the incident radiation absorption chamber was made large enough to accept the entire beam and, yet, only large enough to allow the chamber to operate effectively. The opening for the background chamber was made to match the viewing system opening.

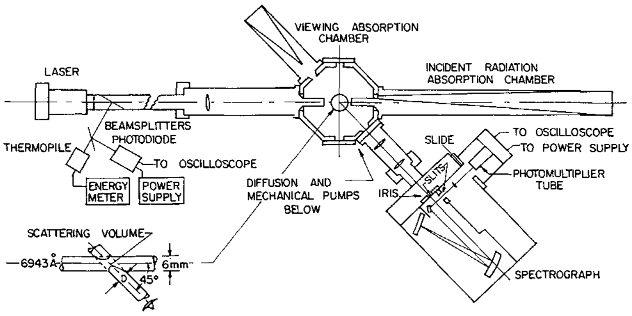

Fig. 2 Schematic of the experimental apparatus.

The design of the optical system was such that a variable scattering volume could be investigated by adjusting an iris, placed at the exit of the optical system. The f number of the optical system was designed to closely match that of the spectrograph (f/4.5). Two achromatic lenses (22 cm focal length) were used. They were placed so that the image and object were at the focal points of the corresponding lenses, thus providing an image to object ratio of one to one. This permitted a system in which parallel light was obtained between the two lenses, where filters could be placed without any distortion of their bandpass characteristics.

The vacuum system is located at the bottom of the test chamber separated from it by a 4-in. vacuum slide valve. The chamber can be pumped down to 10^{-4} torr, as measured with an ionization gage. This was considered to be low enough so that the system would have a minimal amount of impurities even at very low test pressures.

The chamber was designed to accommodate various pressure sensitive instruments as well as a thermometer (0.1°C accuracy) used to record the test gas temperature. The absolute pressure measurements were made utilizing a barometric type manometer. The instrument has an accuracy of 0.1 torr and a scale which can be corrected for changes in room temperature. A baratron was used for absolute pressure measurements below 20 torr.

The distance between the laser and the scattering center were chosen in order to somewhat simulate those distances to be encountered if one would use the technique in one of our aerodynamic simulation facilities. This distance was also large enough so that the image of the laser rod was inside the incident radiation absorption chamber.

Laser System

The system used in these experiments was a TRG Model 104A Ruby Laser System. It can be operated in either a normal or Q-switched mode. In the Q-switched mode the laser output is one joule released in a pulse of 10 nsec duration (measured at the halfwidth). This results in a peak pulse output of approximately 100 megawatts, which was the approximate operating level for most of the experiments herein. The laser head is cooled with room temperature air and emits radiation at a wavelength of 6943 Å, which is linearly polarized in the vertical plane.

The energy output of this system is monitored by a TRG Model 100 Thermopile in conjunction with a calibrated TRG Model 102 energy meter. The pulse shape is monitored by a TRG 105 B photodiode whose output is displayed on a Tektronix 519 oscilloscope. The photodiode has a S-20 spectral response and utilizes a diffusing disk to distribute the light pulse over the entire photosensitive surface. Since the rise time of the photodiode is 0.2 nsec and the rise time of the oscilloscope is 0.29 nsec, the laser pulse, as recorded by this combination, is not substantially distorted. The respective instruments are connected by a special matching 125 ohm, 5-nsec delay cable in order to prevent any ringing of the photodiode circuit.

The monitoring of the laser pulse is accomplished by utilizing two calibrated beamsplitters; one of which reflects a small fraction of the main beam into the other beamsplitter, which in turn reflects and transmits part of this beam into the photodiode and thermopile. Both of these beamsplitters were carefully calibrated utilizing the laser as a source, and two thermopiles, monitoring simultaneously the reflected and transmitted portions of the beam. The thermopile positions were interchanged in order to cross check the calibration.

Spectrograph

The spectrograph available for use in these experiments was a Warner & Swasey Model M-401 Zoom Spectroradiometer. The effective aperture ratio of this instrument is f/4.5. It utilizes a slit assembly which is adjustable from a minimum width of 25μ to a maximum of 1000μ. The instrument has a plane grating whose ruled area of 64×64 mm had 1180 groves/mm and is blazed for 7500 Å. The efficiency of this grating is 74% of the blaze wavelength and approximately 60% at 6500 and 8500 Å. It has a ghost intensity of less than 0.002% in the first order at 5461 Å, and the resolution using a 25μ slit opening is 1.42 Å at 5000 Å.

A high gain photomultiplier (RCA model C31000F) tube, housed in a light sealed container attached to the spectrograph, was utilized to monitor the exit radiation. This tube has good dark current characteristics and has an anode pulse time of 2 nsec at a bias of 2500 v. Its spectral response is depicted in Ref. 5. A highly stabilized, filtered power supply was used to drive the tube, and the variation of the tube gain, as a function of the voltage applied between the anode and cathode, was determined. The absolute gain was determined using a carefully calibrated helium-neon laser as a source.[5]

The output of the tube was displayed on a high-speed Tektronix 454 oscilloscope and recorded on Polaroid film (10,000 ASA speed).

IV. Diagnostic Limitations and System Attenuations

Certain limitations associated with Raman scattering can be outlined briefly. Since the Raman cross sections are very small, a high-intensity source is needed in order to produce scattered light of sufficient intensity which can be recorded above the local background and instrument noise. The use of a source which emits high-intensity radiation at a higher frequency than a ruby laser would be more desirable since the scattered intensity varies with the fourth power of the frequency. This, in conjunction with the fact that the sensitivity of the available photodetectors is much greater in the higher frequency range, would increase the efficiency and range of the technique. Unfortunately, such a high-power source is not presently available. The use of a higher power ruby laser would also increase the intensity of the scattered radiation, thereby, increasing the range of the technique.

Another consideration is the effect of the surrounding molecules on the scattered light. This will manifest itself in the absorption of photons and the subsequent scattering of these Raman photons by the gas between the scattering center and the detector. Subsequent scattering of Raman light will be predominantly of the Rayleigh type due to its large cross section, and therefore, its frequency will be unchanged. The only problem will be that losses will occur since the Raman light is scattered at various angles other than that of the viewing system, and therefore, some will be lost before reaching the detector. When the cross sections involved (either Raman or Rayleigh) are considered, it is realized that any losses due to rescattering will be very small. The amount lost due to absorption will be a function of specific frequency considered. This should also be very small, except when the frequency of the scattered radiation corresponds to a strong absorption band of another specie present in the mixture.

The losses and attenuations introduced by the measurement techniques and system design must now be considered. The system losses manifest themselves mainly in the attenuations and reflections of the incident and scattered radiation by the test gas and optics in the system. These losses can be most easily combined in a calibration factor and were determined utilizing a helium-neon laser (6328 Å) and a very sensitive, calibrated thermopile. The radiation emitted by this laser is polarized in the vertical plane as is the ruby laser used herein. The transmission factor through all of the system optics was measured to be 0.608.

The major instrument losses will be encountered due to the spectrograph, which is used to monitor and measure the separate components of the scattered radiation. Since each of these instruments has its own inherent characteristics as far as losses are concerned, they must be determined in each individual case. The losses are a function of frequency, and therefore, must be known over a range of wavelengths.

In order to minimize these losses, the viewing system optical characteristics should be matched to the particular spectrograph utilized, and the grating should be selected to give the maximum efficiency over the spectral range of interest. The attenuation due to the grating was determined utilizing the data supplied by the manufacturer. The attenuation of any filters which were used in the system was obtained from the transmission curves supplied by the manufacturer. These transmission factors were rechecked utilizing various spectral lamps. The attenuation of the spectrograph was also checked, utilizing the helium-neon laser and was found to agree with the expected attenuation.

In consideration of the aforementioned, one would expect the most severe limitation to be the availability of photodetectors capable of resolving low light intensity levels.

V. Experimental Procedure and Results

As stated in the introduction, the purpose of this investigation is to determine the feasibility of using Raman scattering as a diagnostic technique in order to determine the specie concentration and vibrational temperature of various gases, both in a pure state and in mixtures. As seen in Eq. (2), the intensity of the Raman components vary linearly with specie concentration. It should, therefore, be determined in what range the intensity of the scattered radiation, as recorded in an actual situation, is linear. This would determine, under these experimental conditions, the range in which a measurement of the scattered intensity from a particular specie would provide data from which its concentration could be calculated. This would also provide a calibration curve for each specie which could be utilized to determine the concentration of individual species in a mixture.

The aforementioned was accomplished by filling the chamber with the desired gaseous specie (commercially pure), pulsing the laser and recording the scattered intensity as a function of gas pressure. The pressure (and therefore, the density since the temperature of the test gas remained at room temperature) was subsequently varied over nearly three orders of magnitude. In all tests, the spectrograph was preset at the desired Raman wavelength, and the slit width set at 1000μ. Two filters were placed in the viewing system chamber provided for them. One filter had a narrow reflection band (300 Å), centered at 6943 Å, in order to attenuate the Rayleigh component. It passed all other wavelengths at a slight attenuation ($\approx 25\%$). The second filter has a 100 Å bandpass centered at the desired Raman wavelength and blocked all other wavelengths. This combination provided, in all cases, attenuation of the Rayleigh component of at least five orders of magnitude, while attenuating the Raman component by approximately 50%. The magnitude of the attenuation of the Rayleigh component which is required in any specific application is dependent upon the ghost ratio of the grating utilized, the individual spectrograph characteristics and the ratio of the Rayleigh to Raman intensity.

The utilization of these filters eliminated the possibility that any of the other components would mask the desired Raman component, due to their much greater intensity (Rayleigh Ghosts), or that they would be recorded if one of their higher orders (due to the dispersion of the grating) corresponded to the Raman wavelength being measured. This precaution did not, however, eliminate the possibility of recording radiation of the same frequency as the Raman components, which originated from another source (e.g., if certain wavelengths of the emission spectra of the gas mixture corresponded to some of the Raman wavelengths being observed). In this case, a measurement of the background radiation must be made before any Raman scattering measurements are undertaken and accounted for in the subsequent data reduction. The nonexistence of this background radiation was determined by the subsequent tests described below. The latter considerations are not so important under the present conditions, but they may be important under conditions where there is some substantial background radiation present.

In each test, the incident laser pulse, as well as the scattered intensity, were monitored. Thus, any variation in the laser pulse could be determined and accounted for in the subsequent data reduction.

Pure Gases

This procedure was followed in the testing of pure O_2, N_2 and CO_2 gases; the results of which are shown in Figs. 3–5, respectively. The results obtained utilizing CH_4 are shown and discussed in Ref. 5. Included in each figure is the theoretical linear distribution as given by Eq. (2), as well as the characteristic observation dimension *D*. This dimension, used in conjunction with the beam size, defines the scattering volume observed (refer to the diagram in Fig. 2). In all the tests described herein, the incident beam diameter (6 mm) was kept approximately constant. The results presented in these figures have been nondimensionalized with respect to the intensity of the scattered radiation recorded at a pressure of 760 torr for each specie. This factor is also included in the legend, together with the corresponding incident laser intensity.

Utilization of the previously mentioned slit setting (1000μ), allowed the observation of the entire vibrational-rotational Raman-Stokes band. In the case of carbon dioxide, which has four Raman-Stokes components, the intensity recorded when the spectrograph was utilized was the combined intensity of the vibrational-rotational bands at 7683 and 7696 Å. A separate measurement was made of the combined intensity of the scattered radiation was 8.2 $(10)^{-8}$w, for an incident radiation intensity of 75 Mw.

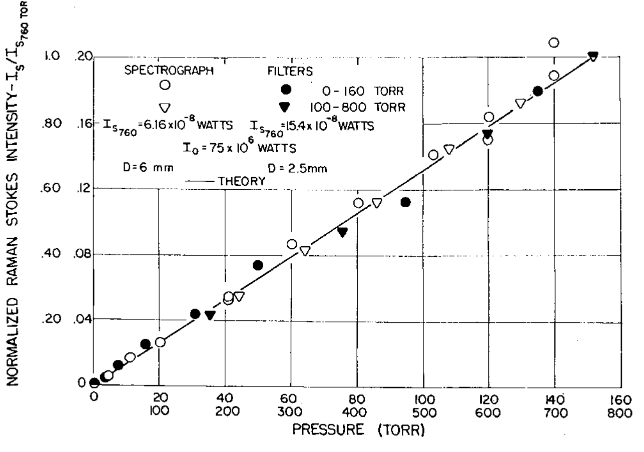

Fig. 3 Measured Raman-Stokes intensity of oxygen (O_2) as a function of pressure. Measured in air at room temperature.

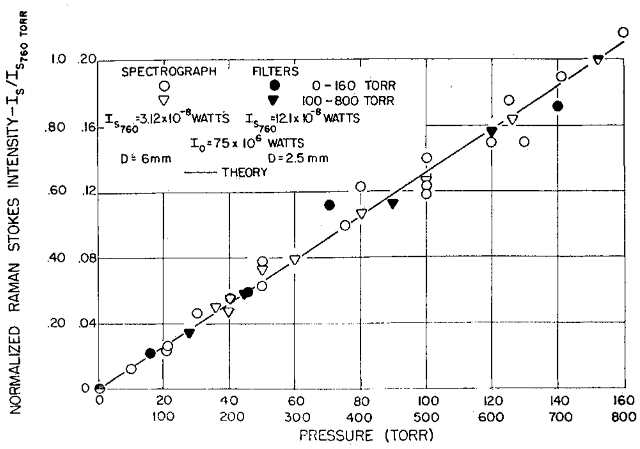

Fig. 4 Measured Raman-Stokes intensity of nitrogen (N_2) as a function of pressure. Measured in air at room temperature.

Good agreement between the measured Raman intensity and theory, over a range of approximately two and one-half orders in magnitude in density, is noticed for all the species. Almost all of the data points fall within 10% of the theoretical line. The accuracy is better at higher pressures and decreases to 15–20% at the lowest pressure. The lower limit for N_2 (10 torr) is higher than O_2 and CO_2 (3–4 torr). This is due to the fact that the Raman scattering cross section of N_2 is smaller than either O_2 or CO_2 and, also, because the phototube is less sensitive at this wavelength. The lower efficiency of the grating and the higher attenuation of interference filters at the longer wavelengths also contribute to this result. A major factor in the determination of these lower density limits is the magnitude of the phototube "noise." That is, at pressures below these limits the intensity of the scattered radiation is within the noise of the phototube, and therefore, is not measurable.

The choice of limiting the measurements to an upper limit of 760 torr was purely based on matters of system integrity and convenience. The upper range of the technique can easily be extended to higher pressures.

As is generally known, the upper limit of the electron beam fluorescence technique is a few torr,[1,2] due to the quenching of the excited molecules.‡ The data as presented here indicate that if Raman scattering from O_2 or CO_2 was used as a diagnostic technique, it is possible to measure densities within the upper bounds of the electron beam technique. The Raman scattering technique, therefore, complements, as well as presents, the possibility of supplementing it with the use of more sensitive phototubes or higher powered lasers.

Included in Figs. 3–5 are the results of tests conducted without the spectrograph, utilizing only narrow bandpass filters to select the proper Raman wavelength. Here, the spectrograph was removed and an iris placed at the image of the scattering volume. In these tests, two narrow reflection band filters, centered at 6943 Å, were used in conjunction with the individual Raman filters. In all cases, this type of filter combination attenuated the Rayleigh component by at least eight orders of magnitude or more.

As in the tests utilizing the spectrograph, measurements were made at very low pressures in order to determine if there was any outside light leakage or background intensity at each wavelength of interest. Tests were also conducted at various

---

‡ This is true if one uses the 1st negative system of nitrogen for diagnostic purposes.

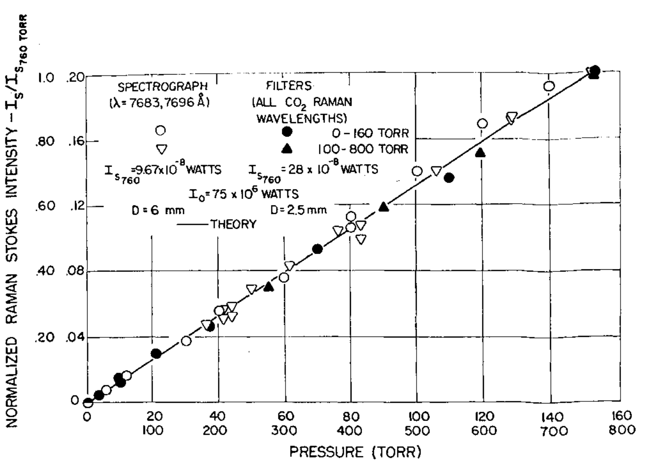

Fig. 5 Measured Raman-Stokes intensity of carbon dioxide (CO_2) as a function of pressure. Measured in air at room temperature.

pressure levels in order to determine if there was any background radiation present. These tests showed the presence of neither. The transmission of any Rayleigh or other radiation through the spectrograph, or through the narrow bandpass filters, was extensively tested and determined to be of such a low magnitude that they were not measurable. Measurements of the Raman scattered intensity were made immediately after filling the chamber as well as after the dust had been allowed to settle. The presence of suspended dust particles was found (within experimental error) not to have any effect on the measurements. As discussed in the Introduction, this result was expected. Only when the wavelength of the scattered Raman radiation from the dust particle is close (i.e., within the resolution of the spectrograph) to the Raman wavelength associated with a gaseous specie of interest, will the presence of dust effect the Raman scattering measurements.

In the test conducted utilizing narrow bandpass filters, the diameter of the iris opening was set at approximately 2.5 mm. The data are presented in the same manner as were the spectrograph data, where the respective nondimensionalization factor is also included in each figure. It should be noticed that in the case of CO_2, all four of the Raman bands were now observed simultaneously.

Since the attenuation of the narrow bandpass filters was much less than that of the spectrograph, it was possible to achieve better spacial resolution at a given pressure, when the filters were utilized, without any sacrifice of the intensity of the scattered radiation. Thus, the scattering volume observed when the narrow bandpass filters were utilized, was reduced to approximately one-fourth that of the volume which was observed when the spectrograph was utilized. As can be seen from these figures, the accuracy of the measurements utilizing either method is about the same.

The relative intensities of the Raman components of the different species considered were checked with that predicted by theory utilizing the experimental values of α' and γ' obtained from the data in Refs. 15 and 16. The comparison was made for the intensities measured using narrow bandpass filters as well as those measured using a spectrograph. These results are presented in Table 1 where good agreement is noticed. Included therein, are the values of α' and $(\gamma'/\alpha')^2$ used to compute the theoretical value of the scattered intensity. It should be pointed out that, in the case of CO_2, the combined intensity of all the Raman-Stokes components was compared to that predicted by theory. It is noticed that intensity measured utilizing the spectrograph is higher than the theoretical value. This probably occurred due to some overlapping of the frequency band resolved when separate measurements of the intensities of 7612, 7623 Å and 7683, 7696 Å bands were made.

The intensity of the O_2 Raman-Stokes component was calculated using Eq. (2) (where C_2 was taken to be $8\pi^4$) and compared to that computed from the scattered radiation trace. The spectrograph measurement was found to be approximately 17% lower than that predicted by theory, whereas the intensity measured utilizing narrow bandpass filters was approximately 10% higher. These differences are within the experimental error resulting from the measurement of each attenuation factor, as well as the estimate of the scattering volume. It also must be remembered that the values of γ' and α' used to predict the theoretical intensity are probably only accurate within 10%. Since the relative intensities agree with that predicted by theory, the differences between the calculated and measured intensity are probably due to the estimate of the scattering volume.

It should be mentioned that the same type of tests were performed using hydrogen as the scattering medium. Unfortunately, due to the very low sensitivity of the phototubes (S-1 and C31000F) at this wavelength, no reliable results could be obtained.

Mixtures

Figures 3–5 can be considered to be calibration curves and, therefore, be used for the investigation of the feasibility of determining individual specie concentrations in various gas mixtures. As stated in the Introduction, the determination of the concentration of an individual specie in a gas mixture should be independent of the type and amount of the other components comprising the mixture. (Here, it is understood that the subsequent rescattering or absorption of the scattered photons by the surrounding molecules is assumed to be negligible (see discussion of limitations).) Thus, the goal of these measurements is the demonstration, under controlled experimental conditions, of the validity of this diagnostic capability.

In these tests, various gases were mixed in known proportions, and the intensity of the various components was recorded. Tests were conducted using a spectrograph and, also, using narrow bandpass filters in order to select the wavelengths of interest.

Measurements were made in order to determine if there was any response for a particular specie when it was not present in the mixture, and the density of other species was high. In all tests the result was negative, indicating that only the intensity of the specific component of interest was recorded. The same type of check was performed when the narrow bandpass filters were utilized. Here, it was found that the CO_2 and O_2 filters each transmitted a very small percentage of the other's component. The amount was measured and used to

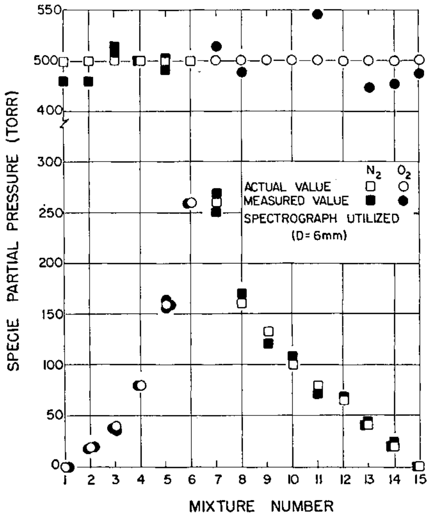

Fig. 6 Specie concentration measurements of O_2 and N_2 in various mixture proportions using a spectrograph.

correct subsequent measurements. This, of course, could be entirely eliminated with the use of filters with a much narrower bandpass.

Initial tests were conducted in two component mixtures (O_2 and N_2) utilizing a spectrograph in order to select the desired wavelength. Here, one component was held at a constant partial pressure, while the other was varied over a range of partial pressures. This would show the relative accuracy of individual specie concentration measurements under various mixture proportions. The results of these tests are shown in Fig. 6. The results are plotted according to the mixture considered, where the ordinate is the individual specie partial pressure. Therefore, the total mixture pressure is obtained by selecting a mixture and adding the various partial pressures indicated by the symbols on or near the vertical line emanating from the desired mixture number. The accuracy of these results are seen to be within those encountered in the pure specie tests.

Other measurements were made involving three component (O_2, N_2 and CO_2) mixtures. These were made utilizing a spectrograph and are presented in Fig. 7. Again, it is seen that each component can be determined with an accuracy equivalent to the pure situation. Mixture number 10 in Fig. 7 shows that species in a three component mixture can be measured with the same degree of accuracy as in the pure tests, even in a mixture where the total mixture pressure is relatively low (60 torr). Mixture number 11 gives the analogous result for a high mixture pressure case (750 torr).

Analogous results were found when narrow bandpass filters were utilized and are shown in Fig. 8. Included herein, are measurements of very small amounts of trace species in high density gas mixtures. The amount of an individual trace specie ranged from approximately 0.4 to 2.5% of the total mixture (see mixture numbers 1–8 in Fig. 8). The error encountered increased as the amount of trace specie was decreased, being approximately 10–15% at partial pressures above 10 torr. This was, of course, expected since this was also the approximate error encountered in the previous tests using pure gases.

All of these measurements indicate that, in a given situation, if the proper precautions have been taken in order to attenuate all other wavelengths, individual specie concentration measurements (and their range) are independent of the density of the other mixture components and are governed "exclusively" by their own individual concentrations. The demonstration of this diagnostic feature was the goal of this aspect of this investigation.

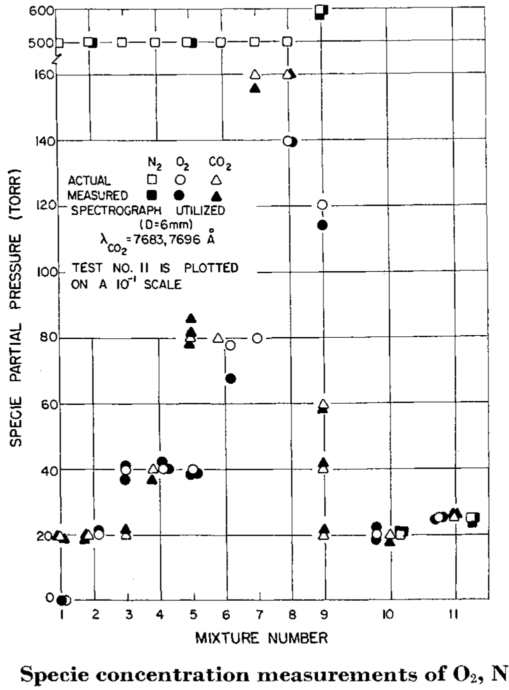

Fig. 7 Specie concentration measurements of O_2, N_2, and CO_2 in various mixture proportions using a spectrograph.

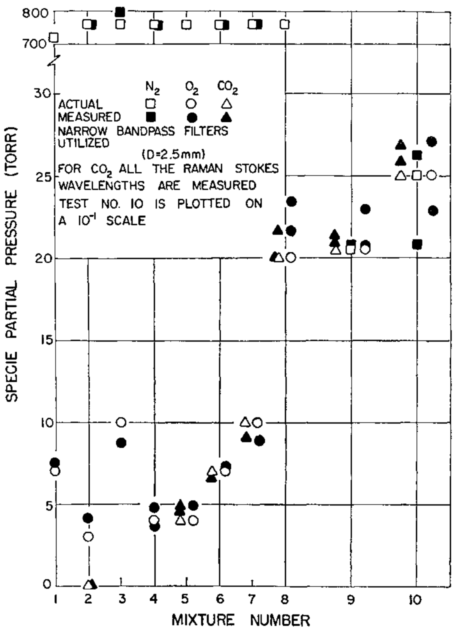

Fig. 8 Specie concentration measurements of O_2, N_2, and CO_2 in various mixture proportions using narrow bandpass filters.

Temperature Measurements

A few tests were conducted in order to determine the feasibility of determining the vibrational temperature of a particular gas by measuring the intensity of the Raman-Stokes and Anti-Stokes components as indicated in Eq. (3). As shown in Ref. 5, the ratio of Raman-Stokes and Anti-Stokes components are on the order of 10^3 to 10^4 at temperatures corresponding to room temperature. The vibrational temperature could, therefore, only be measured for O_2 at 760 torr, since here the ratio was small enough and the signal large enough to allow the measurement of the intensity Anti-Stokes component. Measurements were made using both a spectrograph and narrow bandpass filters.

As is shown in Ref. 5, the sensitivity of the temperature, to the measured intensity ratio, is small at low temperatures and large at high temperatures. This in some way offsets the fact that the intensities of the various Anti-Stokes components are low at low temperatures and, therefore, are subject to more error due to the limited sensitivity of the available phototubes. The vibrational temperature as measured utilizing a spectrograph (D = 6 mm) averages 14% higher than the actual temperature of the gas, while the measurements using narrow bandpass filters (D = 2.5 mm) average to about the correct value. This is probably because of the fact that the intensity recorded using filters is higher, thus, these measurements are less sensitive to the tube "noise" characteristics.

As indicated in Eq. (2), the intensity of the scattered Raman radiation is a function of the temperature of the gas. At low temperatures, this dependence is weak. In any given situation, the simultaneous measurement of I_S and I_A would provide a measurement of the temperature and the concentration. Thus, a calibration made at a lower temperature could be adjusted through the utilization of Eq. (2) and the measured gas temperature. In this case, a calibration which is made at a low temperature can be used as a convenient means of determining the attenuation of the entire system.

Discussion

It has been demonstrated that Raman scattering can be used as a diagnostic technique in order to determine individual specie concentrations in gas mixtures. In a given application, the specie concentration of a particular gas can be determined either using a calibration curve of the type depicted in Figs. 3–5 or utilizing Eq. (2). The utilization of Eq. (2) is more tedious and less accurate since it requires the separate measurement of many attenuation factors and depends upon previously measured quantities such as α' and γ'. It also depends upon a measurement of the scattering volume, a measurement which is very inaccurate at best. The equations should, therefore, be looked upon as giving the appropriate functional dependence of the scattered radiation upon the various governing independent parameters. Thus, any variation in the scattered intensity, due to changes in any of the governing parameters, can be predicted utilizing this equation.

The results which are presented here are dependent upon the experimental arrangement and equipment utilized. A few ways in which either the spatial resolution or density range can be improved are briefly outlined in Ref. 5.

VI. Conclusions

In view of the aforementioned, it may be stated that a technique has been demonstrated which is capable of 1) uniquely identifying individual diatomic (or polyatomic) species in a gas mixture; 2) measuring the concentration of a pure gas over a range of several orders of magnitude in density; 3) measuring the concentration of a particular specie in a gas mixture. This measurement is independent of the density of the other components of the mixture; 4) measuring the vibrational temperature in gases where the number of molecules present in the first vibrational excited state is not insignificant; 5) measuring densities (concentrations) at levels comparable to the upper limit of the electron beam technique; 6) measurements not affected (as in Rayleigh scattering) by the presence of dust particles in the gas; 7) measuring specie concentrations in high velocity flow (due to the shortness of the laser pulse duration); and 8) measurement of local values of a stationary or flowing gas without the influence of disturbing probes.

References

[1] Muntz, E. P., "Measurement of Rotational Temperature, Vibrational Temperature and Molecule Concentration in Non-Radiating Flow at Low-Density Nitrogen," UTIA Rept. 71, 1961, University of Toronto Institute of Aerophysics, Ontario, Canada.

[2] Gadamer, E. O., "Measurement of the Density Distribution in a Rarefied Gas Flow Using the Fluorescence Induced by a Thin Electron Beam," UTIA Rept. 83, March 1962, University of Toronto Institute of Aerophysics, Ontario, Canada.

[3] Sadowsky, C. M. and Vanoverschelde, J. E. H., "The Measurement of Mass Density in a Turbulent Wake by Means of Rayleigh Scattering from a Laser Beam," TN 1764/67, Canadian Armament Research and Development Establishment, Quebec, Canada.

[4] Gerry, E. T. and Rose, D. J., "Plasma Diagnostics by Thompson Scattering of a Laser Beam," *Journal of Applied Physics*, Vol. 37, No. 7, June 1966, pp. 2715–2724.

[5] Widhopf, G. F. and Lederman, S., "Specie Concentration Measurements Utilizing Raman Scattering of a Laser Beam," PIBAL No. 69-46, Nov 1969, Polytechnic Institute of Brooklyn, Farmingdale, N.Y.; also Widhopf, G. F., Ph.D. dissertation, Jan 1970, Dept. of Astronautics, Polytechnic Institute of Brooklyn, Farmingdale, N.Y.

[6] Urtz, R. P., "Plasma Diagnostics Using the Raman Effect," RADC-TDR-64-5, 1964, Rome Air Development Center, Griffiss Air Force Base, N.Y.

[7] Sodha, M. S., Varshni, Y. P., and Daley, J. T., "Spectrographic Detection of Raman Lines; Theory of Plasma Diagnostics Using the Raman Effect," RAC 1195-1, Nov. 1963, Republic Aviation Corp., Farmingdale, N.Y.

[8] Urtz, R. P., "Plasma Specie Probe Techniques," RADC-TR-66-793, 1967, Rome Air Development Center, Griffiss AFB, N.Y.

[9] Cooney, J. A., "Measurement on the Raman Component of Laser Atmosphere Backscatter," *Applied Physics Letters*, Vol. 12, 1968, pp. 40–42.

[10] Garlick, G. F. J., "Luminescence," *Handbuch Der Physik*, Light and Matter II, Vol. XXVI, Springer-Verlag, Berlin, 1958.

[11] Kramers, H. A. and Heisenberg, W. Z., *Physik*, Vol. 31, No. 681, 1925, Springer-Verlag, Berlin, Germany.

[12] Placzek, G., "Rayleigh Strenung and Raman Effect," *Handbuch der Radiologie*, Akademische Verlagegesellshaft VI, Leipzig, Germany, 1934.

[13] Bhagavantam, S., *Scattering of Light and the Raman Effect*, Chemical Publishing Co., New York, 1942.

[14] Herzberg, G., *Spectra of Diatomic Molecules*, Van Nostrand, New York, 1945.

[15] Yoshino, T. and Bernstein, H. J., "Intensity in the Raman Effect, VI The Photoelectrically Recorded Raman Spectra of Some Gases," *Journal of Molecular Spectroscopy*, Vol. 2, 1958, pp. 213–239; also, private communication with H. J. Bernstein, Oct. 1968.

[16] Standsbury, E. J., Crawford, M. F., and Welsh, H. L., "Determination of Rates of Change of Polarizability from Raman and Rayleigh Intensities," *Canadian Journal of Physics*, Vol. 31, 1953, pp. 954–961.